INTERNATIONAL ATOMIC ENERGY AGENCY
UNITED NATIONS EDUCATIONAL, SCIENTIFIC AND CULTURAL ORGANIZATION
INTERNATIONAL CENTRE FOR THEORETICAL PHYSICS
I.C.T.P., P.O. BOX 586, 34100 TRIESTE, ITALY, CABLE: CENTRATOM TRIESTE

UNITED NATIONS INDUSTRIAL DEVELOPMENT ORGANIZATION

INTERNATIONAL CENTRE FOR SCIENCE AND HIGH TECHNOLOGY
c/o INTERNATIONAL CENTRE FOR THEORETICAL PHYSICS 34100 TRIESTE (ITALY) VIA GRIGNANO, 9 (ADRIATICO PALACE) P.O. BOX 586 TELEPHONE 040-224572 TELEFAX 040-224575 TELEX 460449 APH I

SMR/760-52

"College on Atmospheric Boundary Layer and Air Pollution Modelling"
16 May - 3 June 1994

"Estimation of Atmospheric Boundary Layer Parameters for Diffusion Applications"

A.P. VAN ULDEN
Royal Netherlands Meteorological Institute
de Bilt, The Netherlands

Please note: These notes are intended for internal distribution only.

Estimation of Atmospheric Boundary Layer Parameters for Diffusion Applications

A. P. VAN ULDEN AND A. A. M. HOLTSLAG

Royal Netherlands Meteorological Institute, De Bilt, the Netherlands

(Manuscript received 11 June 1984, in final form 26 March 1985)

ABSTRACT

This paper gives the outline of a "meteorological preprocessor" for air pollution modeling. It is shown how significantly more information can be extracted from routinely available measurements than the traditional Pasquill stability classes and power law wind speed profiles. Also it is shown how additional special measurements—if available—can be accommodated. The methods are primarily intended for application in generally level, but not necessarily homogeneous terrain. The improved characterization of the state of the planetary boundary layer allows a more modern and probably more accurate description of diffusion. The paper is an extended version of an introductory paper presented during the "Workshop on Updating Applied Diffusion Models" in Clearwater, Florida, January 1984.

1. Introduction

The quality of a dispersion model is strongly influenced by its meteorological input. Therefore the meteorological input has to comprise the meteorological factors that have a direct effect on the dispersion of a pollutant that is emitted in the atmosphere. These factors are the vertical profiles of

1) *wind:* determines where the pollutant goes and how fast;
2) *atmospheric turbulence:* determines turbulent dispersion;
3) *temperature:* affects the rise of a buoyant plume.

Since these meteorological factors are not usually measured at the location and time where we want to apply the dispersion model, a "meteorological preprocessor" is needed to estimate the required meteorological input from available measurements.

Current regulatory models normally use very simplified meteorological input. They use Pasquill–Gifford–Turner stability classes, which are only valid over land with small roughness and which only crudely characterize the state of the atmospheric surface layer. Therefore these classes are strongly biased toward neutral stability while higher up the boundary layer can be significantly stable or unstable.

They also use power-law representations of the wind profile with powers that are only a function of the stability class. Turning of the wind with height is neglected. There is overwhelming evidence that the wind speed profile is not properly described by a power law and that significant turning of the wind with height occurs, mainly in stable conditions.

They do not account explicitly for the effect of temperature stratification on plume rise.

There is clear evidence that improvement of the meteorological input can also improve the quality of dispersion calculations. Examples are the use of convective scaling in the unstable boundary layer (Deardorff, 1970; Nieuwstadt, 1980; Briggs, 1983; Baerentsen and Berkowicz, 1981), the use of local scaling in the stable boundary layer (Hunt, 1982; Nieuwstadt, 1984a,b; Venkatram *et al.*, 1984) and the use of surface layer similarity for dispersion from surface releases (van Ulden, 1978; Horst, 1979; Gryning *et al.*, 1983).

There is also evidence that the meteorological input can be improved by the use of better meteorological preprocessors. It is the purpose of this paper to summarize recent developments of "preprocessors" and to provide guidance to those who want to obtain better meteorological input from existing routine measurements.

In this paper we limit ourselves to dry boundary layers, i.e. to boundary layers in which no significant amounts of clouds or fog are present.

2. Atmospheric boundary layer parameters

The physical basis for the meteorological preprocessors that we will describe in this paper is provided by parameterizations of the structure of the atmospheric boundary layer (ABL) including its interaction with the ground. General discussions on this subject can be found in McBean (1979), Nieuwstadt and van Dop (1982), and Pasquill and Smith (1983). Here we restrict ourselves to a brief listing of the main characteristic parameters, their definition and their physical meaning. We will use three primary ABL parameters: i.e. the ABL depth h, the surface heat flux H_0 and the surface momentum flux τ_0. These parameters deter-

mine a number of secondary parameters which will be given below.

• h: The ABL depth h is defined as the depth of the fully turbulent boundary layer near the ground. In this layer mixing is much more rapid than above it. Therefore it is often called the mixing layer.

• H_0: The surface heat flux is the vertical flux of sensible heat that is transferred by turbulence to or from the surface. The parameter H_0 determines the heating or cooling of the ABL, directly affects the temperature profile and indirectly the depth of the ABL. Also, due to the action of gravity, the heat flux gives rise to buoyant production or destruction of turbulent kinetic energy. This production is given by

$$B_0 = gH_0/(\rho C_p T), \tag{1}$$

where g is the acceleration of gravity, ρ the air density, C_p the specific heat of air and T the absolute temperature. When B_0 is positive, turbulence is created by buoyancy. In this case B_0 and h define a convective velocity scale

$$w_* = (B_0 h)^{1/3}. \tag{2}$$

This is the turbulent velocity scale in the unstable ABL and forms the basis for convective scaling of dispersion.

• τ_0: The surface momentum flux or shear stress defines the friction velocity

$$u_* = (\tau_0/\rho)^{1/2}, \tag{3}$$

where u_* determines the shear production of turbulence kinetic energy at the surface. This is given by

$$S_0 = u_*^3/(kz_0), \tag{4}$$

where $k \approx 0.4$ is the van Kármán constant and z_0 the surface roughness length. Furthermore u_* is the velocity scale for turbulence in the near-neutral and stable boundary layer. The heat flux and u_* together define a temperature scale:

$$\theta_* = -H_0/(\rho C_p u_*), \tag{5}$$

where θ_* is a temperature scale for turbulent heat transfer, while $g\theta_*/T$ is a scale for turbulent buoyancy transfer.

The last important ABL parameter is the Obukhov length which is defined by

$$L = u_*^2/(kg\theta_*/T). \tag{6}$$

From (1), (4), (5) and (6) it follows that

$$-z_0/L = B_0/S_0. \tag{7}$$

Thus $-z_0/L$ is a stability measure that gives the relative importance of the surface production of turbulence by buoyancy and by shear.

In all we have now introduced three length scales i.e., z_0, L and h; two velocity scales, i.e., u_* and w_*; and one temperature scale, i.e., θ_*. These scales form the basis for the main existing similarity theories for the ABL.

3. Estimation of u_* and θ_* with the profile method

a. *Profile method*

In the absence of turbulence measurements we have to derive u_*, θ_* and L from other available data. This can be done with use of the Monin-Obukhov theory for the atmospheric surface layer.

The basic equations are the following. According to surface-layer similarity theory, u_* and θ_* can be written as functions of the vertical profiles of windspeed $U(z)$ and potential temperature $\theta(z)$ (McBean, 1979):

$$u_* = kU(z)/[\ln(z_1/z_0) - \psi_M(z_1/L) + \psi_M(z_0/L)], \tag{8}$$

and

$$\theta_* = k[\theta(z_3) - \theta(z_2)]/[\ln(z_3/z_2) - \psi_H(z_3/L) + \psi_H(z_2/L)]. \tag{9}$$

In these equations ψ_M and ψ_H are stability functions and z_1–z_3 are arbitrary heights in the surface layer. The function ψ_M is discussed in Section 6. The term ψ_H is given by (Dyer, 1974; Yaglom, 1977; Businger *et al.*, 1971; Wieringa, 1980a,b):

$$\psi_H = 2\ln\left(\frac{1+y^2}{2}\right),$$

where

$$y = (1 - 16z/L)^{1/4}, \quad \text{for} \quad L < 0, \tag{9a}$$

and

$$\psi_H = -5z/L, \quad \text{for} \quad L > 0. \tag{9b}$$

The similarity profiles (8) and (9) are valid typically for $z_0 \ll z < L$ (e.g., Businger *et al.*, 1971; Dyer, 1974; Yaglom, 1977).

When measurements are available of a single wind speed at z_1 and a single temperature difference between z_3 and z_2, we can solve for u_*, θ_*, and L by iteration. This is called the profile method (Nieuwstadt, 1978; McBean, 1979; Berkowicz and Prahm, 1982a).

Also, estimates of T and z_0 are needed; T need not be known accurately (say within 10 K) and estimation procedures for z_0 are described in the next section. Since the similarity profiles are only valid for $z_0 \ll z \leqslant L$ and L is regularly as small as 10 m, it is advisable to restrict the application of the profile method to measurements over terrain with a low roughness at heights less than 10 m. The profile method is a reliable method for estimating the surface parameters, provided the temperature difference is measured accurately and preferably over a great height interval (e.g., 2 m–10 m).

b. *Estimation of the surface-roughness length z_0*

The surface-roughness length z_0 is an important parameter in the integral flux-profile relation of the atmospheric surface layer given by (8) and (9). Moreover z_0 forms the lower boundary in diffusion models (e.g.,

Pasquill and Smith, 1983). The length z_0 represents, in principle, the roughness characteristics of a homogeneous terrain or landscape. Very often, however, we have relatively smooth terrain disturbed by occasional obstructions or by large perturbations. In such cases an effective roughness length was found appropriate for use in the flux-profile relations (e.g., Nieuwstadt, 1978; Beljaars, 1982).

When an effective roughness length is used, surface fluxes can be derived that are representative for a larger area than local derived fluxes. This is important, for instance, for the estimation of the wind profile at greater heights from surface fluxes and single wind speed. This is demonstrated by Korrell *et al.* (1982) for the Boulder tower and by Beljaars (1982) and Holtslag (1984) for the Cabauw tower. Furthermore the horizontal velocity fluctuations scale on a friction velocity scale are representative for a larger area (Beljaars *et al.*, 1983).

The value of the effective roughness length can be obtained from a method described by Wieringa (1976, 1980a,b, 1983). This method relates the surface roughness length to the normalized standard deviation of wind speed (σ_u/U). Alternatively, we can use the normalized maximum gust. The latter method is suitable for routine station applications, when gust records are available. The value of z_0 with Wieringa's method is representative for an area of about 5 km^2 (Beljaars, 1982).

When no gust records are available we can obtain a crude value for the effective roughness length from a visual terrain description. In Table 1 we have adopted the Davenport classes as given by Wieringa (1980). For the application of Table 1 we can define wind direction sectors as needed to distinguish between major variations in upwind terrain conditions. Sectors less than 20° in width are not expected to be suitable in practice.

TABLE 1. Terrain classification by Davenport (1960) and Wieringa (1980) in terms of effective surface roughness length z_0.

Class	Brief terrain description	z_0 (m)
1	Open sea, fetch at least 5 km	0.0002
2	Mud flats, snow; no vegetation, no obstacles	0.005
3	Open flat terrain; grass, few isolated obstacles	0.03
4	Low crops; occasional large obstacles, $x/H^* > 20$	0.10
5	High crops; scattered obstacles, $15 < x/H^* < 20$	0.25
6	Parkland, bushes; numerous obstacles, $x/H^* \sim 10$	0.5
7	Regular large obstacle coverage (suburb, forest)	(1.0)
8	City center with high- and low-rise buildings	?–?

* Here x is typical upwind obstacle distance and H the height of the corresponding major obstacles. Class 8 is theoretically intractable within the framework of boundary layer meteorology and can better be modeled in a wind tunnel. For simple modeling applications it may be sufficient to use only classes 1, 3, 5, 7 and perhaps 8.

In practice the roughness length often is estimated from wind profiles observed in neutral stability conditions. However, as discussed by Wieringa (1981) and Beljaars (1982) for a rough to smooth transition, the turbulence adjusts more slowly to the underlying surface than the wind profile. For that reason the upwind roughness averages over larger distances can be better evaluated from σ_u/U or gustiness than from profiles. Conversely, this means that only above a certain height can the wind profile be described with the effective roughness length. Beljaars (1982) estimates this height as 2δ, where δ is the height of the major obstacles. Closer to the surface the flux-profile relations differ from those over uniform terrain (Beljaars *et al.*, 1983).

4. Estimation of u_* and θ_* with the energy budget method

In the profile method we have used that θ_* can be written as an implicit function of a vertical temperature difference $\Delta\theta$ and u_*, i.e., $\theta_* = f_1(\Delta\theta, u_*)$. When no vertical temperature difference is available for the application of (9), this information can be replaced by information on the surface energy budget:

$$H_0 + \lambda E = Q^* - G, \tag{10}$$

where λE is the latent heat flux (λ is the latent heat of water vaporization and E is the evaporation), Q^* is the net radiation and G the soil heat flux. An example for a clear day is shown in Fig. 1. $H_0 + \lambda E$ is the energy flux that is supplied to or extracted from the air, while $Q^* - G$ is the source or sink for this energy. Using $H_0 = -\rho C_p u_* \theta_*$, (10) can be written as

$$\theta_* = \frac{\lambda E - Q^* + G}{\rho C_p u_*}. \tag{11}$$

In this equation λE, Q^* and G can be parameterized (as we will see later) in terms of the total cloud cover N, the solar elevation ϕ, the air temperature T, the friction velocity u_* and θ_* itself. The idea is to use (11) to write θ_* as a function of the variables N, ϕ, T and u_*:

$$\theta_* = f_2(N, \phi, T, u_*). \tag{12}$$

This equation then replaces (9). The further procedure of finding θ_* and u_* from (8) and (12) by iteration is similar to that used in the profile method. In the following sections we will discuss the modeling of λE, Q^* and G as well as the resulting functions of the type (12).

a. *Modeling of the evaporation*

The evaporation is formally given by the Penman-Monteith equation (Monteith, 1981), which can be written as

$$\lambda E = \frac{\delta S}{1 + \delta S}(Q^* - G) + \frac{\delta \rho \lambda \Delta q}{(1 + \delta S) r_a}. \tag{13}$$

In this equation $\delta = r_a/(r_a + r_c)$, r_a is the aerodynamic

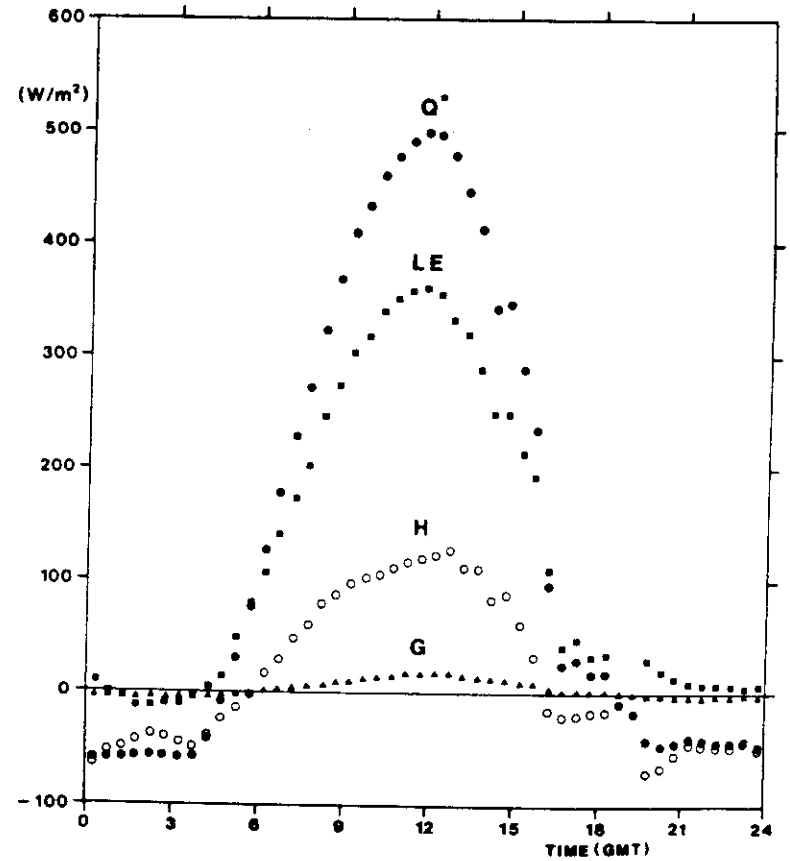

FIG. 1. Components of the surface energy budget measured at Cabauw, the Netherlands on 31 May 1978.

resistance for the transfer of heat and water vapor from the surface to the air and r_c the surface resistance for the transfer of water from soil and vegetation to the surface; formally $r_a = (T - T_0)/(\theta_* u_*)$, where T and T_0 are the temperatures of the air and of the surface respectively. The slope of the saturation enthalpy curve is $S = \partial(\lambda q_s)/\partial(C_p T)$ and q_s the saturation specific humidity; the humidity deficit of the air is $\Delta q = q_s(T) - q$, where q is the specific humidity of the air.

The first term at the right-hand side of (13) may be called the thermodynamic evaporation, since it is directly related to the external energy source $Q^* - G$. The last term in (13) we call the aerodynamic evaporation, since it is the additional evaporation due to the action of wind. In practice the two terms are of the same order of magnitude. For a direct evaluation of (13) a measurement of Δq is needed as well as estimates of r_a and r_c. Attempts to do so in a practical manner have been made by, e.g., Smith and Blackall (1979), Deheer-Amissah *et al.* (1981) and Berkowicz and Prahm (1982a). These attempts show that such an evaluation is quite complicated. There is however, a simple alternative: the modified Priestley–Taylor (1972) model (de Bruin and Keijman, 1979; van Ulden and Holtslag, 1983). This model is based on the experience that both the thermodynamic and the aerodynamic evaporation are strongly correlated with the so-called equilibrium evaporation:

$$\lambda E_e = \frac{S}{1 + S}(Q^* - G). \tag{14}$$

This is the evaporation that would occur when the surface is wet ($r_c = 0$, $\delta = 1$) and the air saturated ($\Delta q = 0$).

The correlation between the thermodynamic evaporation and λE_e is directly clear. The correlation of the aerodynamic term and λE_e is caused by the fact that λE_e and Δq have a similar diurnal cycle (de Bruin and Holtslag, 1982). Therefore it is useful to split Δq into a part Δq_e that is correlated with λE_e and a part Δq_d that is not correlated. Using this, we may parameterize the evaporation as (de Bruin and Holtslag, 1982; van Ulden and Holtslag, 1983):

$$\lambda E = \alpha\left[\frac{S}{S + 1}(Q^* - G) + \beta\rho\lambda\Delta q_d u_*\right], \tag{15}$$

where α and β are empirical coefficients. In the first term between brackets we have absorbed that part of the aerodynamic evaporation that is due to Δq_e. The usefulness of (15) for predicting the evaporation has been shown by de Bruin and Holtslag (1982) for day-

time applications and indirectly by van Ulden and Holtslag (1983) for nighttime applications. The discussion on the values of α, β and Δq_d is postponed till later.

b. Modeling the net radiation

The net radiation consists of the net shortwave radiation K^* that originates from the sun and the net longwave radiation L^*, i.e., the difference between the outgoing radiation L^- from the earth surface and the incoming radiation L^+ from the atmosphere. Thus

$$Q^* = K^* + L^+ - L^-. \tag{16}$$

The net shortwave radiation can be parameterized as:

$$K^* = (a_1 \sin\phi + a_2)(1 - b_1 N^{b_2})(1 - r). \tag{17}$$

Here $a_1 \sin\phi + a_2$ is the incoming solar radiation with clear skies and a_1 and a_2 are empirical coefficients. Typical values are $a_1 = 990$ W m^{-2} and $a_2 = -30$ W m^{-2} (Haurwitz, 1945; Lumb, 1964; Collier and Lockwood, 1975; Kasten and Czeplak, 1980; Holtslag and van Ulden, 1983). The reduction factor $1 - b_1 N^{b_2}$ gives the interception of solar radiation by clouds with b_1 and b_2 empirical coefficients. Typical values are b_1 0.75 and $b_2 = 3.4$ (Kasten and Czeplak, 1980). The reduction factor $(1 - r)$ is due to the reflection of incoming solar radiation by the surface, where r is the reflection factor or albedo. A typical value for a vegetated surface is $r = 0.23$ (Monteith and Szeicz, 1961).

The application of (17) is limited to $\phi > 1.7°$. For smaller values $K^* = 0$ should be used. The accuracy of (17) ranges from about 50 W m^{-2} with clear skies to about 90 W m^{-2} for cloudy skies (Holtslag and van Ulden, 1983). If more accurate results are needed, measurements of the solar radiation are recommended.

The incoming longwave radiation can be parameterized as (Swinbank, 1963; Arnfield, 1979; Paltridge and Platt, 1976):

$$L^+ = c_1 \sigma T_r^6 + c_2 N \tag{18}$$

where $\sigma = 5.67 \times 10^{-8}$ W m^{-2} K^{-1} is the Stefan-Boltzmann constant, T_r is the air temperature at a reference height z_r; $c_1 = 9.35 \times 10^{-6}$ K^{-2} and $c_2 = 60$ W m^{-2} are empirical coefficients. The first term at the right-hand side gives the contribution of the gaseous atmosphere (mainly water vapor and carbon dioxide). The second term gives the contribution of clouds (N is the fraction of the sky that is covered with clouds). According to Swinbank (1964) the reference height z_r should be taken above the layer in which strong temperature gradients occur. Van Ulden and Holtslag (1983) found $z_r = 50$ m a suitable choice.

The outgoing longwave radiation is given by the Stefan-Boltzmann law:

$$L^- = \sigma T_0^4, \tag{19}$$

where the earth's surface is assumed to be a black body (Sellers, 1965) and T_0 is the radiation temperature of the surface. Since we are only interested in the net longwave radiation we decompose (19) as $L^- = \sigma T_r^4 - 4\sigma T_r^3 (T_r - T_0)$, which with (18) yields

$$L^+ - L^- = L_i^* + 4\sigma T_r^3 (T_r - T_0), \tag{20}$$

where

$$L_i^* = -\sigma T_r^4 (1 - c_1 T_r^2) + c_2 N \tag{21}$$

is called the isothermal net longwave radiation. This is the net longwave radiation that would occur when the atmospheric surface layer was isothermal (i.e., $T_r - T_0 = 0$).

The last term in (20) is a correction factor that accounts for the temperature differences that normally occur over the atmospheric surface layer. Since typically $4\sigma T_r^3 = 5$ W m^{-2} K^{-1} and $|T_r - T_0|$ can be as large as 10 K, the correction factor can be as large as ± 50 W m^{-2}. In comparison with (typically) $L_i^* = -90$ W m^{-2} this correction is quite significant.

The correction factor is not normally measured, so it should be parameterized. During daytime it is strongly correlated with Q^* (Monteith and Szeicz, 1961). Holtslag and van Ulden (1983) found

$$4\sigma T_r^3 (T_r - T_0) = -C_H Q^*, \tag{22}$$

where C_H is an empirical heating coefficient that can be approximated by:

$$C_H = 0.38\left[\frac{(1 - \alpha)S + 1}{S + 1}\right]. \tag{23}$$

During the nighttime $T_r - T_0$ is strongly affected by wind speed. In this case surface layer similarity can be used to eliminate $T_r - T_0$:

$$T_r - T_0 = \frac{\theta_*}{k}\left[\ln\left(\frac{z_r}{z_H}\right) + 5\frac{z_r}{L}\right] - \Gamma_d z_r, \tag{24}$$

where $\Gamma_d = 0.01$ K m^{-1} is the dry adiabatic lapse rate and where the surface reference height for heat z_H is used instead of z_0 because near the surface the resistance for heat transfer differs from that for momentum transfer (Garratt and Hicks, 1973). For short grass, typically, $(1/k)\ln(z_r/z_H) = 30$ (van Ulden and Holtslag, 1983).

c. Modeling the soil heat flux

The soil heat flux is the downward heat flux that leaves the radiation level, passes through a layer of air and vegetation and goes into the ground. Because the layer of air and vegetation has a high resistance and a low heat capacity the soil heat flux should be strongly correlated with the temperature difference over this layer. Furthermore this temperature difference should be strongly correlated with the temperature difference $(T_r - T_0)$ in the air, because both differences vary mainly with the diurnal cycle of T_0. For these reasons a plausible parameterization for G is

$$G = -A_G (T_r - T_0), \tag{25}$$

where A_G is an empirical coefficient for the soil heat transfer. For a grass surface, van Ulden and Holtslag (1983) propose $A_G = 5$ W m^{-2} K^{-1}. With this value they obtained a satisfactory simulation of the nighttime energy balance. The same value may be retrieved from the work of de Bruin and Holtslag (1982) for daytime applications. So (25) is a useful approximation for grass, both for nighttime and for daytime. The temperature difference in (25) is eliminated as in Section 4b. For daytime this leads to

$$G = C_G Q^*, \tag{26}$$

where

$$C_G = (A_G/4\sigma T_r^3)C_H. \tag{27}$$

d. Definition of daytime and nighttime

The results of the preceding sections may now be combined to give the desired equations for θ_*. The first step in the procedure is the estimation of the isothermal net radiation

$$Q_i^* = K^* + L_i^*, \tag{28}$$

where K^* and L_i^* are estimated with (17) and (21). In this equation L_i^* is only a weak function of the temperature T_r and for practical applications we may as well use estimations with a typical mean nighttime 50 m temperature, perhaps $T_r = 283$ K. For this temperature (28) reduces to

$$Q_i^* = K^* - 91 + 60N. \tag{29}$$

This equation is used in the first place to discriminate between daytime cases when $Q_i^* > 0$ and nighttime cases when $Q_i^* < 0$.

e. Practical equations for θ_* during daytime

For daytime the θ_* equation is obtained from (11), (15), (16), (20), (22), (26) and (28). The result can be written as

$$\theta_* = -\frac{[(1-\alpha)S + 1](1 - C_G)Q_i^*}{(S+1)(1 + C_H)\rho C_p u_*} + \alpha\theta_d, \tag{30}$$

where C_H and C_G are given by (23) and (27) and

$$\theta_d = \beta\lambda\Delta q_d/C_p, \tag{31}$$

is an empirical temperature scale. This temperature scale can be estimated from the data by de Bruin and Holtslag (1982). These authors found that $\beta\rho\lambda\Delta q_d u_* \approx 20$ W m^{-2}. With a typical value of $u_* = 0.5$ m s^{-1} (during daytime) and $\rho = 1.2$ kg m^{-3} this leads to $\theta_d = 0.033$. From the same data it followed that for normal wet grass in a moderate climate the moisture parameter $\alpha = 1$. For "Prairie Grass" conditions (Barad, 1958) with rather dry vegetation, Holtslag and van Ulden (1983) found that typically $\alpha = 0.5$. In this case the same estimate for θ_d can be used as before. For dry bare soil α vanishes. We further need an estimate for slope S of the saturation enthalpy curve. For $270 < T_r < 310$ K this slope can be quite well approximated by:

$$S = \exp[0.055(T_r - 279)]. \tag{32}$$

f. Practical equations for θ_* during nighttime

For nighttime, θ_* is obtained from (11), (15), (16), (20), (24), (25) and (28). The result is a quadratic equation in θ_*. The solution of this equation can be written as:

$$\theta_* = T_r\{[(d_1 v_*^2 + d_2 v_*^3)^2 + d_3 v_*^2 + d_4 v_*^3]^{1/2} - d_1 v_*^2 - d_2 v_*^3\}, \tag{33}$$

where

$$v_* = u_*/(5gz_r)^{1/2}, \tag{34}$$

$$d_1 = \frac{1}{2k}\ln\frac{z_r}{z_h}, \tag{35}$$

$$d_2 = \tfrac{1}{2}(1 + S)\rho C_p(5gz_r)^{1/2}/(4\sigma T_r^3 + A_G), \tag{36}$$

$$d_3 = -Q_i^*/(4\sigma T_r^4 + A_G T_r) + \Gamma_d z_r/T_r, \tag{37}$$

$$d_4 = (1 + S)\rho C_p(5gz_r)^{1/2}\theta_d/(4\sigma T_r^4 + A_G T_r), \tag{38}$$

and where $\alpha = 1$ has been used. In these equations we further use as typical values: $z_r = 50$ m, $d_1 = 15$, $A_G = 5$ W m^{-2} K^{-1} and $\theta_d = 0.033$ K. With these values the coefficients d_2, d_3 and d_4 still depend on the reference temperature T_r, while d_3 also depends on N and K^*.

For practical applications we again neglect the T_r dependence and approximate the constants by their values for $T_r = 283$ K. We then obtain (using $z_r = 50$ m, $(1/k)\ln(z_r/z_H) = 30$, $\theta_d = 0.033$) the values $(5gz_r)^{1/2} = 50$ m s^{-1}, $d_1 = 15$, $d_2 = 6600$, $d_4 = 1.55$ and

$$d_3 = (-K^* + 96 - 60N)/2870, \tag{39}$$

where the dry-adiabatic correction term has been absorbed in Q_i^*. The relation between θ_* and u_* for these constants is compared with data for $K^* = 0$ in Fig. 2. It is seen that the general behavior of (33) is satisfactory. Also, the present results agree with the mean value $\theta_* = 0.08$ found by Venkatram (1980) for predominantly clear sky conditions. The advantage of the present approach is that solutions for θ_* and u_* are also obtained for low wind speed, provided the wind profile described in Section 6 is used. Thus, in principle, the present method also gives a practical solution for very stable conditions. That such practical solutions are useful has been shown by Holtslag (1984).

Another advantage of the present method is that no special provisions have to be made for transition hours between day and night.

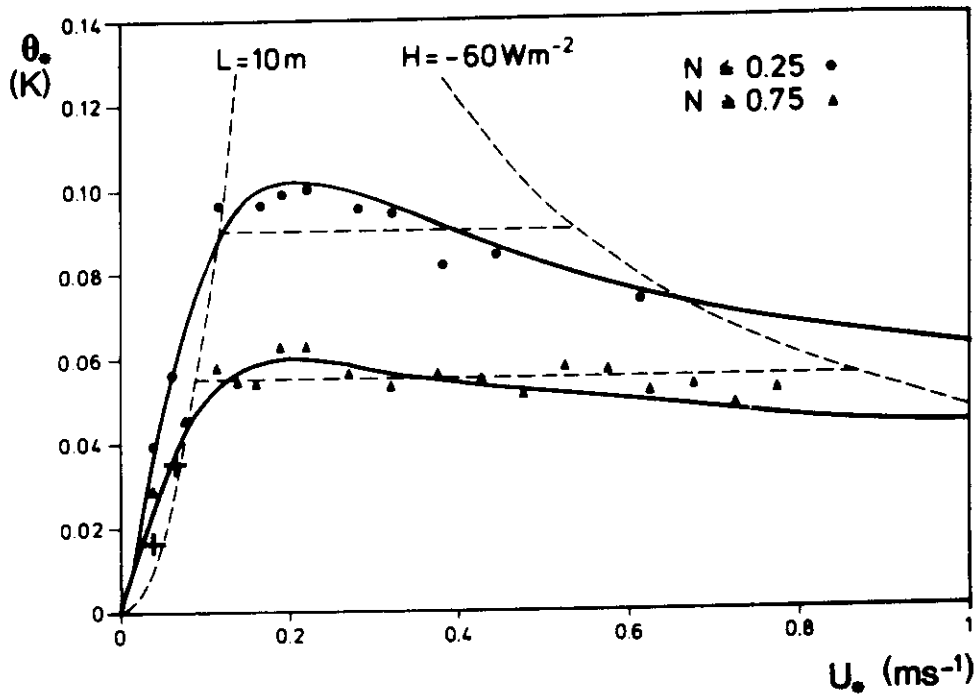

FIG. 2. The variation of θ_*(K) with u_* (m s^{-1}) for two classes of total cloud cover N. Dots refer to profile measurements with clear skies, triangles to measurements with cloudy skies. Plus signs refer to sonic anemometer measurements. Each data point represents the average of at least 15 half-hourly runs. The solid lines are computed with Eqs. (32)–(38) with $K^* = 0$. The curves $L = 10$ m and $H = -60$ W m^{-2} are given for reference. The measurements were made at Cabauw.

5. Mixing height and temperature profile

a. *The neutral ABL*

The depth of the fully neutral stationary ABL follows from asymptotic similarity theory (Blackadar and Tennekes, 1968):

$$h_n = c_n u_*/f, \tag{40}$$

where f is the Coriolis parameter and $c_n = 0.2$ an empirical constant. This relation indicates that in neutral conditions the mixing depth varies only with wind speed. In practice, however, often elevated inversion layers exist even when a major part of the ABL can be considered neutral. In that case the ABL depth is limited by the height of the elevated inversion. When observations are available that indicate the presence of an inversion at a height less than that given by (40), the inversion height should be taken as ABL depth instead of (40). Further the use of (40) should be limited to atmospheric conditions that are sufficiently neutral. A practical rule of thumb is the requirement $|u_*/(fL)| < 4$. This corresponds crudely with $|h/L| < 1$.

b. *The stable ABL*

The structure of the stable ABL is best illustrated by some typical examples of measured temperature profiles as are shown in Figs. 3 and 4 (Cabauw measurements taken from van Ulden and Wessels, 1973). Figure 3 shows the development of the temperature profile

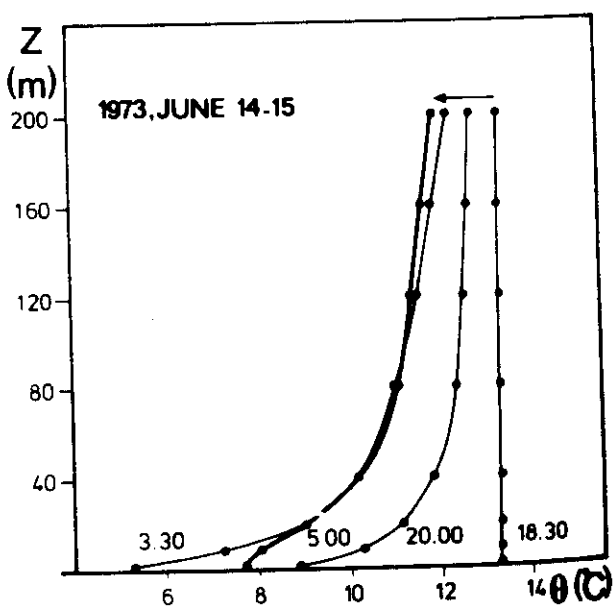

FIG. 3. The temperature profile measured in Cabauw on a clear night with a low wind speed: U (200 m) $\approx$ 1 m s^{-1} for indicated times (U.T.).

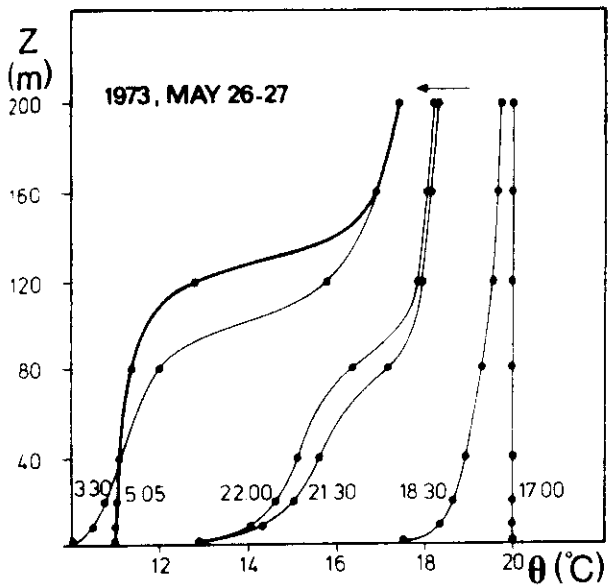

FIG. 4. As in Fig. 3, but with U (200 m) $\approx$ 10 m s^{-1}. At time t = 5.05 U.T. $H_0 = 0$.

for a clear night with a low wind speed [U (200 m) $\approx$ 1 m s^{-1}]. In such nights no fully developed turbulent boundary layer is present and cooling occurs due to radiation divergence and some weak intermittent turbulence. The vertical potential temperature gradient is seen to decrease monotonously with height. The profile resembles strongly the exponential profile proposed by Stull (1983) or the cubic profile by Yamada (1979).

Figure 4 shows a clear night with a moderate wind speed [U (200 m) $\approx$ 10 m s^{-1}]. In this case a fully turbulent boundary layer is maintained by wind shear. The early development of the shape of the temperature profile is similar as in the light wind case. However, after a few hours a triple structure develops. Near the surface a layer is present in which the temperature gradient decreases with height (up to about 40 m). Then a bulk layer follows in which the temperature gradient *increases* with height. On top of this layer an interfacial layer is present in which again the temperature gradient decreases with height. The latter layer marks the transition from fully turbulent to laminar flow. The maximum wind speed is usually observed at the top of the bulk layer, i.e., near the height with the greatest temperature gradient. This observed triple structure resembles somewhat the structure of the model by Wetzel (1982). He, however, assumed a linear bulk layer. Although this is an oversimplification, Wetzel's model seems adequate for practical applications when only crude temperature profiles are needed.

Wetzel's model requires an independent estimate of the depth of the turbulent layer. For this, two main types of diagnostic equations have been proposed. The first is a bulk Richardson expression (Hanna, 1969; Wetzel, 1982).

$$h_s = \frac{\mathrm{Ri}_b T U_h^2}{g(\theta_h - \theta_0)}. \tag{41}$$

Here $\mathrm{Ri}_b \approx 0.33$ is a Richardson number to be assumed constant, U_h is the wind speed at the top of the ABL, $\theta_h - \theta_0$ is the potential temperature difference over the ABL. Although (41) has proven to be an acceptable estimate for h, it has the disadvantage that $\theta_h - \theta_0$ and especially U_h is not normally available. Therefore (41) is less suitable for practical applications.

More suitable is Zilitinkevich's (1972) expression:

$$h_s = c_s(u_* L/f)^{1/2}, \tag{42}$$

where $c_s \approx 0.4$ is an empirical coefficient. Recently Nieuwstadt (1984a,b) provided some theoretical support for this expression and also showed that it gives an acceptable fit to data. An example of the use of (42) is given in Fig. 5.

Equation (42) offers problems at high wind speeds and low θ_* values, because L may become quite large. Therefore in practice it is advisable to limit h by its neutral value (40) in cases for which (42) gives higher values than (40). This corresponds with the requirement earlier mentioned that the neutral estimate should be taken when $|u_*/(fL)| < 4$.

c. *The unstable ABL*

Also the unstable ABL has a triple structure. In this case the surface layer has a negative temperature gradient. It is again described by surface layer similarity. In the bulk layer the potential temperature is approximately constant with height. The interfacial layer has a positive temperature gradient. It can be characterized by a temperature jump $\Delta\theta$ and a layer thickness Δh.

For the depth of the unstable ABL no adequate diagnostic equations exist; instead, rate equations are needed (e.g., Carson, 1972; Tennekes, 1973; Stull, 1983; Deardorff *et al.*, 1974). The practical applicability of such models is discussed, e.g., in Tennekes and van Ulden, 1974; Driedonks, 1982; Reiff *et al.*, 1984; Driedonks and Tennekes, 1984. The main equations may be summarized as follows:

The rate equation for h is

$$\partial h/\partial t = w_h + w_e, \tag{43}$$

where w_h is the mean vertical velocity of the air at the height h and w_e the entrainment velocity. While w_h can be estimated from convergence calculations, it is often neglected; w_e follows from

$$w_e/w_m = c_f(c_i + \mathrm{Ri}_m), \tag{44}$$

where

$$w_m = (w_*^3 + c_r u_*^3)^{1/3} \tag{45}$$

is a velocity scale,

$$\mathrm{Ri}_m = gh\Delta\theta/(T w_m^2) \tag{46}$$

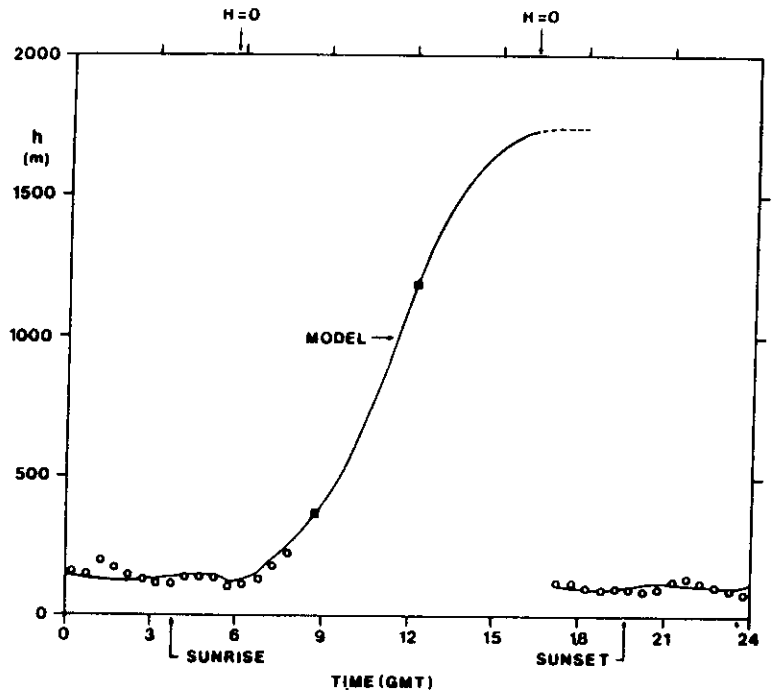

FIG. 5. The depth of the boundary layer in Cabauw on 31 May 1978. Circles give solar measurements (Nieuwstadt, 1984). Squares give values derived from radiosoundings. Solid line is computed from Eq. (41) for the stable period and from Eqs. (42)–(47) for the unstable period. The method of Section 4 has been used for estimating u_* and θ_*.

is a bulk Richardson number and $c_f = 0.2$, $c_t = 1.5$ and $c_\tau = 25$ are empirical coefficients.

The temperature jump at the top of the ABL is calculated with

$$\partial(\Delta\theta)/\partial t = \gamma w_e - \partial\bar{\theta}/\partial t, \tag{47}$$

where $\gamma = \partial\theta/\partial z$ is the temperature gradient above the ABL and $\bar{\theta}$ the mean potential temperature of the ABL; γ is obtained from measurements at the beginning of the day and $\partial\bar{\theta}/\partial t$ is given by

$$\partial\bar{\theta}/\partial t = (1 + c_f)H_0/\rho C_p h. \tag{48}$$

The set equations (43)–(48) can be solved numerically to provide the development of h and $\Delta\theta$. An example is shown in Fig. 5.

The thickness Δh of the interfacial layer has been discussed by Deardorff *et al.* (1980) for convective conditions ($c_\tau u_*^3 \ll w_*^3$). The result for Δh can be written in the present notation as:

$$\Delta h \Big/ \left(h - \tfrac{1}{2}\Delta h\right) = c_0 + c_i/\mathrm{Ri}_m, \tag{49}$$

where $c_0 = 0.21$ and $c_i = 1.31$ are empirical coefficients. The use of (49) in cases with nonzero u_* is only tentative. From (47) and (49) a crude estimate for the temperature gradient in the interfacial layer is obtained as:

$$(\partial\theta/\partial z)_i \approx \Delta\theta/\Delta h. \tag{50}$$

This estimate can be used for the estimation of buoyant plume penetration in the interfacial layer (Willis and Deardorff, 1984; Manins, 1979).

6. The wind profile

Normally the wind speed in the boundary layer increases with height, while at the same time a clockwise turning occurs in the Northern Hemisphere. In this section we will describe methods for estimating these effects from surface observations and an estimated ABL depth. Other information like the geostrophic wind or upper air wind observations are not dealt with.

a. The turning of the wind with height

The turning of the wind with height is an important feature for air pollution modeling, because it affects both the direction in which the pollution goes, and the lateral dispersion. Unfortunately little is known about directional wind shear. Some information can be extracted from a paper by Holtslag (1984). In Table 2 observed data on the turning of the wind with height are given. In unstable and near-neutral conditions the turning is small below 200 m. In stable conditions a mean turning angle up to 40° is observed. The data from the table can be ordered by using a scaled height z/h, where h is computed as described in Section 5. It

TABLE 2. Turning of the wind with height. The mean difference D and the rms difference σ_D are corrected for the bias D of the observed wind direction at height z and the 20 m height. Observed Cabauw data taken from Holtslag (1984). A distinction is made in 9 classes of stability, ranging from very unstable a to neutral d and very stable i. For each class the mean Obukhov length $L_m = 1/(\overline{1/L})$ is given. Also for the neutral and stable classes d–h the mean ABL depth $h = 1/(\overline{1/h})$ is given, where h is computed as described in Section 5.*

	Class								
Parameter	*a*	*b*	*c*	*d*	*e*	*f*	*g*	*h*	*i*
L_m (m)	−30	−100	−370	10^4	350	130	60	20	(9)
h_m (m)				1000	330	220	160	120	(100)
				z = 40 m					
D	0	0	0	1	2	4	5	7	12
σ_D	2	2	2	2	2	4	3	4	5
				z = 80 m					
D	4	3	3	4	7	11	16	21	24
σ_D	8	6	5	6	7	9	10	12	12
				z = 120 m					
D	8	6	5	6	10	17	24	29	31
σ_D	13	12	7	8	8	11	14	14	14
				z = 160 m					
D	10	8	7	9	14	22	30	34	36
σ_D	17	16	11	12	10	16	18	17	17
				z = 200 m					
D	12	10	9	12	18	28	35	38	39
σ_D	17	18	14	12	11	17	21	18	20

* The values of L_m and h_m for class i are tentative values obtained by fitting profile functions to observed wind profiles up to 200 m. The value of h_m is not given for the unstable classes, because of the high variability of h within each class; typical values range from 500 m–2000 m. Note that a positive value of D refers to a clockwise change in wind direction with increasing height. Data are given in degrees.

appears that all data on the mean turning angle are described within a few degrees by

$$D(z)/D(h) = d_1[1 - \exp(-d_2 z/h)], \qquad (51)$$

where $D(z)$ is the turning angle at the height z, $D(h)$ at the height h and $d_1 = 1.58$, $d_2 = 1.0$ are empirical coefficients. From the data for the stable classes a turning angle $D(h) = 35°$ can be derived. This corresponds with $D(h) - D(z = 10\text{ m}) \approx 32°$.

Since (51) has been derived from observations between 20 and 200 m the use of it close to the surface should be avoided. The scatter around the mean turning angle as given by (51) is quite large. At 200 m the rms error ranges from about 12° in near neutral conditions to about 19° in stable and unstable cases. Nevertheless, the mean correction (51) is significant especially in stable conditions.

b. *The wind speed profile*

The basis for wind speed profile calculations is the Monin-Obukhov similarity theory for the surface layer as given formally by (8). For the present purpose we rewrite (8) as:

$$U(z) = U(z_1)\frac{\left[\ln\left(\frac{z}{z_0}\right) - \psi_M\left(\frac{z}{L}\right)\right]}{\left[\ln\left(\frac{z_1}{z_0}\right) - \psi_M\left(\frac{z_1}{L}\right)\right]}, \qquad (52)$$

where z_1 is the height at which a wind observation is available and where we have omitted the small terms $\psi_M(z_0/L)$. The most commonly used ψ_M stability functions are (Dyer, 1974; Yaglom, 1977; Businger *et al.*, 1971; Wieringa, 1980a,b; Paulson, 1970):

$$\psi_M = 2\ln\left(\frac{1+x}{2}\right) + \ln\left(\frac{1+x^2}{2}\right) - 2\tan^{-1}(x) + \pi/2, \qquad (52a)$$

where

$$x = (1 - 16z/L)^{1/4}, \quad \text{for} \quad L < 0, \qquad (52b)$$

and

$$\psi_M = -5z/L, \quad \text{for} \quad L > 0. \qquad (52c)$$

Strictly speaking, these functions are valid for $z_0 \ll z < |L|$. It appears, however, that in unstable conditions (52) in combination with (52a), (52b) can be used at

heights $z \gg |L|$, maybe even up to $z = h$ (Garratt *et al.*, 1982; Holtslag, 1984). Equations (52a) and (52b) can also be replaced by a more simple function (Jensen *et al.*, 1984):

$$\psi_M = (1 - 16z/L)^{1/4} - 1. \quad (53)$$

This function has the same performance as (52a, b) for $0 < -z/L < 30$. When applied to the Cabauw data as described by Holtslag (1984), starting from a measured wind at 10 m, total cloud cover N and solar elevation ϕ and using the energy budget method described in Section 4 for estimating u_* and θ_*, (52) and (53) appear to predict the wind speed at 200 m with an accuracy ranging from 20% in near-neutral conditions to 30% in very unstable conditions. At 80 m the errors are about half this large.

In stable conditions, (52) in combination with (52c) fails for $z > L$ (Webb, 1970; Hicks, 1976; Carson and Richards, 1978; Holtslag, 1984). Equation (52c) can, however, be replaced by another empirical function that has the same performance for $z < L$, but a much better performance for $z > L$. This function is:

$$\psi_M = -17[1 - \exp(-0.29z/L)]. \quad (54)$$

For small z/L this function reduces to the linear stability function (52c) while at large z/L it has the same behavior as the modified stability functions proposed by Holtslag (1984) and Carson and Richards (1978). A function similar to (54) has been proposed by Petersen *et al.* (1984). The performance of (54) even in very stable conditions is remarkable. When applied to the Cabauw data set (Holtslag, 1984) and using Section 4 for estimating u_* and θ_*, it appears to predict the wind speed up to 200 m without significant systematic errors even in cases in which h is well below 200 m. The scatter, however, is not insignificant. The rms error at 200 m ranges from 20% in near neutral conditions to 30% in very stable conditions. At 80 m the errors are about half this large.

7. Conclusions

We have described methods for estimating, from local routine measurements, the boundary layer parameters that are relevant for air pollution modeling. For the surface parameters a comprehensive synthesis is made of existing parameterizations, with an emphasis on the surface energy balance. For the wind speed profile recent empirical similarity functions are proposed that are both simple and effective. A new similarity function for the turning of the wind with height is proposed. For the daytime mixing height, widely accepted rate equations are adopted. For the temperature gradient of the capping inversion a tentative procedure is given. Crude methods for the depth and temperature profile of the stable boundary layer are taken from the literature, which are probably an advancement over current practice in air pollution modeling.

REFERENCES

André, J. C., 1983: On the variability of the nocturnal boundary layer depth. *J. Atmos. Sci.*, **40**, 2309–2311.

Arnfield, A. J., 1979: Evaluation of empirical expressions for the estimation of hourly and daily totals of atmospheric longwave emissions under all sky conditions. *Quart. J. Roy. Meteor. Soc.*, **105**, 1045–1052.

Baerentsen, J. H., and R. Berkowicz, 1984: Monte Carlo simulation of plume dispersion in the convective boundary layer. *Atmos. Environ.*, **18**, 701–712.

Barad, M. L. (Ed.), 1958: Project Prairie grass, a field program in diffusion. Geophys. Res. Rep. No. 59, Vols. I and 2, Geophysics Research Directorate. 489 pp.

Beljaars, A. C. M., 1982: The derivation of fluxes from profiles in perturbed areas. *Boundary-Layer Meteorol.*, **24**, 35–55.

——, P. Schotanus and F. T. M. Nieuwstadt, 1983: Surface layer similarity under non-uniform fetch conditions. *J. Climate Appl. Meteor.*, **22**, 1800–1810.

Berkowicz, R., and L. P. Prahm, 1982a: Evaluation of the profile method for estimation of surface fluxes of momentum and heat. *Atmos. Environ.*, **16**, 2809–2819.

——, and ——, 1982b: Sensible heat flux estimated from routine meteorological data by the resistance method. *J. Appl. Meteor.*, **21**, 1845–1864.

Blackadar, A. K., and H. Tennekes, 1968: Asymptotic similarity in neutral barotropic planetary boundary layers. *J. Atmos. Sci.*, **25**, 1015–1020.

Briggs, G. A., 1983: Diffusion modeling with convective scaling and effects of surface inhomogeneities. *Speciality Conf. on Air Quality Modeling of the Urban Boundary Layer*, Baltimore, Amer. Meteor. Soc., (unpublished).

Businger, J. A., J. C. Wyngaard, Y. Izumi and E. F. Bradley, 1971: Flux-profile relationships in the atmospheric surface layer. *J. Atmos. Sci.*, **28**, 181–189.

Carson, D. J., 1973: The development of a dry inversion-capped convectively unstable boundary layer. *Quart. J. Roy. Meteor. Soc.*, **99**, 450–467.

——, and J. R. Richards, 1978: Modelling surface turbulent fluxes in stable conditions. *Boundary-Layer Meteorol.*, **14**, 67–81.

Collier, L. R., and J. G. Lockwood, 1974: The estimation of solar radiation under cloudless skies with atmospheric dust. *Quart. J. Roy. Meteor. Soc.*, **100**, 678–681.

de Bruin, H. A. R., and A. A. M. Holtslag, 1982: A simple parameterization of the surface fluxes of sensible and latent heat during daytime compared with the Penman-Monteith concept. *J. Appl. Meteor.*, **21**, 1610–1621.

——, and J. Q. Keijman, 1979: The Priestley–Taylor evaporation model applied to a large shallow lake in the Netherlands. *J. Appl. Meteor.*, **18**, 898–903.

Deardorff, J. W., 1970: Convective velocity and temperature scales for the unstable planetary boundary layer and for Rayleigh convection. *J. Atmos. Sci.*, **27**, 1211–1213.

——, G. E. Willis and B. H. Stockton, 1980: Laboratory studies of the entrainment zone of a convectively mixed layer. *J. Fluid Mech.*, **100**, 41–46.

Deheer-Amissah, A., U. Högström and A. S. Smedman-Högström, 1981: Calculation of sensible and latent heat fluxes and surface resistance from profile data. *Boundary-Layer Meteorol.*, **20**, 35–49.

Driedonks, A. G. M., 1982: Models and observations of the growth of the atmospheric boundary layer. *Boundary-Layer Meteorol.*, **23**, 283–306.

——, and H. Tennekes, 1984: Entrainment effects in the well-mixed atmospheric boundary layer. *Boundary-Layer Meteorol.*, **30**, 75–105.

Dyer, A. J., 1974: A review of flux-profile relationships. *Boundary-Layer Meteorol.*, **7**, 363–372.

Garratt, J. R., and B. B. Hicks, 1973: Momentum, heat and water vapour transfer to and from natural and artificial surfaces. *Quart. J. Roy. Meteor. Soc.*, **99**, 680–687.

——, J. C. Wyngaard and R. J. Francey, 1982: Winds in the at-

mospheric boundary layer—Prediction and observation. *J. Atmos. Sci.*, **39**, 1307–1316.

Gryning, S. E., A. P. van Ulden and S. Larsen, 1983: Dispersion from a continuous ground-level source investigation by a K model. *Quart. J. Roy. Meteor. Soc.*, **109**, 355–364.

Hanna, S. R., 1969: The thickness of the planetary boundary layer. *Atmos. Environ.*, **3**, 519–536.

Haurwitz, B., 1945: Insolation in relation to cloudiness and cloud density. *J. Meteor.*, **2**, 154–166.

Hicks, B. B., 1976: Wind profile relationships from the 'Wangara' experiment. *Quart. J. Roy. Meteor. Soc.*, **102**, 535–551.

Holtslag, A. A. M., 1984: Estimates of diabatic wind speed profiles from near surface weather observations. *Boundary-Layer Meteorol.*, **29**, 225–250.

——, and A. P. van Ulden, 1983: A simple scheme for daytime estimates of the surface fluxes from routine weather data. *J. Climate Appl. Meteor.*, **22**, 517–529.

Horst, T. W., 1979: Lagrangian similarity modeling of vertical diffusion from a ground-level source. *J. Appl. Meteor.*, **18**, 733–740.

Hunt, J. C. R., 1982: Diffusion in the stable boundary layer. *Atmospheric Turbulence and Air Pollution Modelling*, F. T. M. Nieuwstadt and H. van Dop, Eds., Reidel, 231–274.

Jensen, N. O., E. L. Petersen and I. Troen, 1984: Extrapolation of mean wind statistics with special regard to wind energy applications. *WMO World Climate Programme*, Rep. WCP-86, 85 pp.

Kasten, F., and G. Czeplak, 1980: Solar and terrestrial radiation dependent on the amount and type of cloud. *Solar Energy*, **24**, 177–189.

Korrell, A., H. A. Panofsky and R. J. Rossi, 1982: Wind profiles at the Boulder tower. *Boundary-Layer Meteorol.*, **22**, 295–312.

Lumb, F. E., 1964: The influence of cloud on hourly amounts of total solar radiation at the sea surface. *Quart. J. Roy. Meteor. Soc.*, **90**, 43–56.

Manins, P. C., 1979: Partial penetration of an elevated inversion layer by chimney plumes. *Atmos. Environ.*, **13**, 733–741.

McBean, G. A. Ed., 1979: *The planetary boundary layer*. Tech. Note No. 165, WMO 530, 201 pp.

Monteith, J. L., 1981: Evaporation and surface temperature. *Quart. J. Roy. Meteor. Soc.*, **107**, 1–27.

——, and G. Szeicz, 1961: The radiation balance of bare soil and vegetation. *Quart. J. Roy. Meteor. Soc.*, **87**, 159–170.

Nieuwstadt, F. T. M., 1978: The computation of the friction velocity u_* and the temperature scale T_* from temperature and wind velocity profiles by least-square methods. *Boundary-Layer Meteorol.*, **19**, 235–246.

——, 1980: Application of mixed layer similarity to the observed dispersion from a ground-level source. *J. Appl. Meteor.*, **19**, 157–162.

——, 1984a: The turbulent structure of the stable, nocturnal boundary layer. *J. Atmos. Sci.*, **41**, 2202–2216.

——, 1984b: Some aspects of the turbulent stable boundary layer. *Boundary-Layer Meteorol.*, **30**, 31–55.

——, and H. van Dop, 1982: *Atmospheric Turbulence and Air Pollution Modelling*. Reidel, 358 pp.

Obukhov, A. M., 1971: Turbulence in an atmosphere with a non-uniform temperature. *Boundary-Layer Meteorol.*, **2**, 7–29.

Paltridge, G. W., and C. M. R. Platt, 1976: *Radiative Processes in Meteorology and Climatology. Development in Atmospheric Science, Vol. 5*. Elsevier, 318 pp.

Pasquill, F., and F. B. Smith, 1983: *Atmospheric Diffusion*. Third ed., Wiley, 437 pp.

Paulson, C. A., 1970: The mathematical representation of wind speed and temperature profiles in the unstable atmospheric surface layer. *J. Appl. Meteor.*, **9**, 856–861.

Petersen, E. L., I. Troen and J. W. Wieringa, 1984: Development of a method for wind climate analysis for non-mountainous terrain in Europe. *European Wind Energy Conf.*, Hamburg.

Priestly, C. H. B., and R. J. Taylor, 1972: On the assessment of surface heat flux and evaporation using large scale parameters. *Mon. Wea. Rev.*, **106**, 81–92.

Reiff, J., D. Blaauboer, H. A. R. De Bruin, A. P. van Ulden and G. Cats, 1984: An air mass transformation model for short-range weather forecasting. *Mon. Wea. Rev.*, **112**, 393–412.

Sellers, W. D., 1965: *Physical Climatology*. The University of Chicago Press, 272 pp.

Smith, F. B., and R. M. Blackall, 1979: The application of field experiment data to the parameterization of the dispersion of plumes from ground level and elevated sources. *Mathematical Modelling of Turbulent Diffusion in the Environment*, J. Harris, Ed., Academic Press, 201–238.

Stull, R. B., 1973: Inversion-rise model based on penetrative convection. *J. Atmos. Sci.*, **30**, 1092–1099.

——, 1983: A heat-flux history length scale for the nocturnal boundary layer. *Tellus*, **35A**, 219–230.

Swinbank, W. C., 1963: Longwave radiation from clear skies. *Quart. J. Roy. Meteor. Soc.*, **89**, 339–348.

——, 1964: Discussion on the 1963 article. *Quart. J. Roy. Meteor. Soc.*, **90**, 488–493.

Tennekes, H., 1973: A model for the dynamics of the inversion above a convective boundary layer. *J. Atmos. Sci.*, **30**, 558–567.

——, and A. P. van Ulden, 1974: Short term forecasts of temperature and mixing height on sunny days. *Preprints 2nd Symp. on Atmos. Turbulence, Diffusion and Air Quality*, Santa Barbara, Amer. Meteor. Soc., 35–40.

van Ulden, A. P., 1978: Simple estimates of vertical diffusion from sources near the ground. *Atmos. Environ.*, **12**, 2121–2129.

——, and H. R. A. Wessels, 1973: Profiles of temperature and horizontal visibility measured on a 200 m meteorological mast. Paper presented at *Symp. on the Atmospheric Boundary Layer*, Mainz, (unpublished).

——, and A. A. M. Holtslag, 1983: The stability of the atmospheric surface layer during nighttime. Preprints *Sixth Symp. on Turbulence and Diffusion*, Boston, Amer. Meteor. Soc., 257–260.

Venkatram, A., 1980: Estimating the Monin-Obukhov length in the stable boundary layer for dispersion calculations. *Boundary-Layer Meteorol.*, **19**, 481–485.

——, D. Strimaitis and D. Discristofaro, 1984: A semiempirical model to estimate vertical dispersion of elevated releases in the stable boundary layer. *Atmos. Environ.*, **18**, 923–928.

Webb, E. K., 1970: Profile relationships: The log-linear range and extension to strong stability. *Quart. J. Roy. Meteor. Soc.*, **96**, 67–90.

Wetzel, P., 1982: Toward parameterization of the stable boundary layer. *J. Appl. Meteor.*, **21**, 7–13.

Wieringa, J., 1976: An objective exposure correction method for average wind speeds measured at a sheltered location. *Quart. J. Roy. Meteor. Soc.*, **102**, 241–253.

——, 1980a: A revaluation of the Kansas mast influence on measurements of stress and cup-anemometer overspeeding. *Boundary-Layer Meteorol.*, **18**, 411–430.

——, 1980b: Representativeness of wind observations at airports. *Bull. Amer. Meteor. Soc.*, **51**, 962–971.

——, 1981: Estimation of mesoscale and local-scale roughness for atmospheric transport modelling. *11th Int. Tech. Meeting on Air Pollution Modelling and its Application*, Plenum, 279–295 pp.

——, 1983: Description requirements of non-ideal wind stations—for example, Aachen. *J. Wind Engin. Industr. Aerodyn.*, **11**, 121–131.

Willis, G. E., and J. W. Deardorff, 1983: On plume rise within the convective boundary layer. *Atmos. Environ.*, **17**, 2435–2447.

Yaglom, A. M., 1977: Comments on wind and temperature flux-profile relationships. *Boundary-Layer Meteorol.*, **11**, 89–102.

Yamada, T., 1979: Prediction of the nocturnal surface inversion height. *J. Appl. Meteor.*, **18**, 526–531.

Zilitinkevich, S. S., 1972: On the determination of the height of the Ekman boundary layer. *Boundary-Layer Meteorol.*, **3**, 141–145.